Muon spin relaxation

In an ingenious application of parity violation, physicists are measuring interstitial magnetic fields and diffusion in solids by analyzing the anisotropy in the decay of injected spin-polarized positive muons.

Robert H. Heffner and Donald G. Fleming

Since its discovery in 1957, parity violation in the weak interaction has occupied both experimental and theoretical physicists in a broad effort directed toward its understanding. One manifestation of parity violation is found in the decay of spin-polarized muons. In the earliest searches for suitable stopping materials for studying the weak interaction through the decay of positive muons, physicists noticed that the muon polarization remaining after thermalization depends markedly on the nature of the stopping environment, varying from about 10% in some liquids such as benzene to 100% in most metals. Data of this nature contained the beginnings of the technique of muon spin relaxation, also known as muon spin resonance or muon spin rotation. In this technique, which is akin to magnetic resonance, one monitors the spin polarization of muons to learn about the materials into which they have been injected. Muon spin relaxation now constitutes a significant research effort at the world's meson-producing accelerators: at Brookhaven and LAMPF in the United States, Dubna and Leningrad in the Soviet Union, CERN and SIN in Switzerland, TRIUMF in Canada, KEK in Japan and NIKHEF in the Netherlands.

In a typical muon spin relaxation experiment, a beam of positive spin-polarized muons stops in the material of interest, and muons reach thermal equilibrium at interstitial positions in the lattice. As in magnetic resonance, the spin polarization of the muon is then modulated or decreased by its interactions with the local magnetic environment. One can detect this effect of the local magnetic environment with great sensitivity by monitoring the spatial anisotropy of the decay of the muon, which emits a positron preferentially along the muon spin direction in a classic example of parity violation. These decay positrons are easy to detect using conventional counter technology (figure 1) over time windows ranging from a few nanoseconds to tens of microseconds. This gives muon spin techniques a range of applicability complementary to conventional nuclear magnetic resonance and electron paramagnetic resonance spectroscopies.

Although developed by scientists trained in nuclear and particle physics, muon spin techniques now attract both physicists and chemists working in such diverse fields as radiation chemistry, reaction dynamics, atomic and molecular physics, nuclear and particle physics and condensed-matter physics. This broad interest in "applied muon physics," is amply manifest in recent papers and review articles[1–5] as well as in the published proceedings[6] of three international conferences on the topic. Unfortunately, space does not permit discussion of all of the fields here. We will focus on condensed-matter physics, which accounts for about three-quarters of the world's effort in muon spin relaxation. Also for brevity's sake, we will concentrate on experiments that use positive muons—studies using neg-

Robert Heffner is a research scientist at the Los Alamos Meson Physics Facility at Los Alamos National Laboratory, in New Mexico. Donald Fleming is professor of chemistry at the University of British Columbia, in Vancouver.

0031-9228 / 84 / 1200 38-09 / $01.00

Muon spin relaxation spectrometer at LAMPF. The black scintillation counters slide through an opening in the Helmholtz coils. A dilution-refrigerator cryostat containing the sample material slides into the Helmholtz coils from the opposite side. The beam enters from behind the spectrometer, which is set up in the transverse field geometry illustrated in figure 2. Figure 1

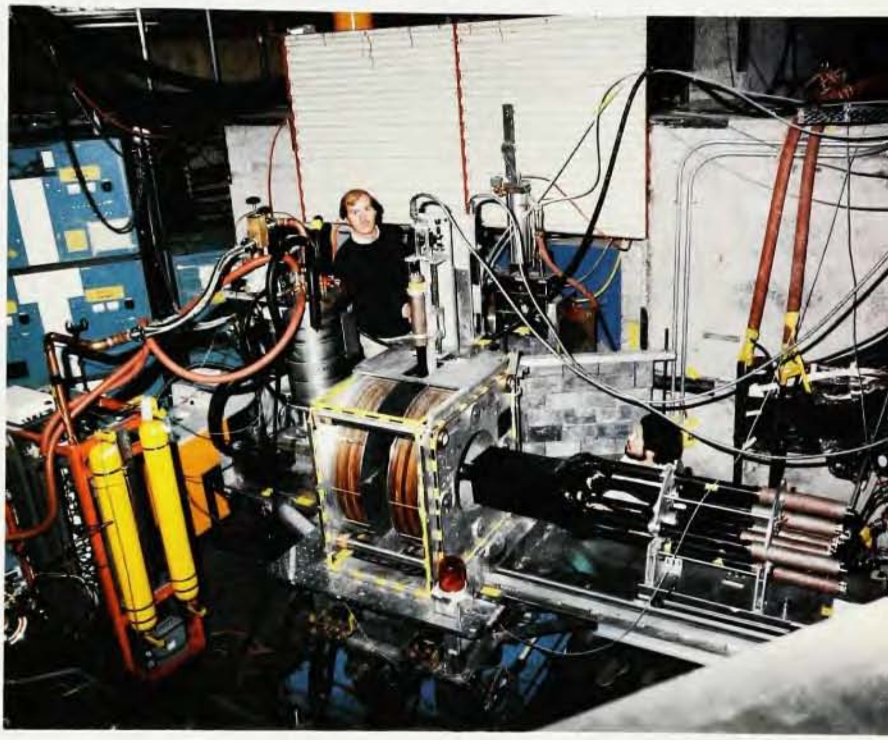

ative muons are based on the same principles.

Advantages and disadvantages. The positive muon has three fundamental properties that make it very useful for studying condensed matter—its mass, which is only one-ninth that of the proton, its point charge and its large magnetic moment. The positive muon may bind with an orbital electron and form a simple impurity atom μ^+e^- called muonium; this is particularly true in nonmetallic targets such as gases, liquids and semiconductors. The positive muon acts in matter just as a light proton (not as a heavy electron), and we can regard the muonium atom as an ultralight isotope of hydrogen. In studies of diffusion and chemical reaction dynamics, the positive muon and muonium are therefore uniquely sensitive probes of many aspects of quantum tunneling. Recent and definitive results have come from studies of simple metals, notably copper and aluminum, and from studies of chemical dynamics in gases.

The positive muon by itself is free of the core atomic electrons characteristic of nuclear or atomic probes possessing a greater nuclear charge. Therefore one can study the magnetic fields produced by conduction electrons in a lattice, which are drawn to the positive muon, without side effects caused by these electron cores; the positive muon thus is a sensitive probe for the study of interstitial magnetism. Because of the muon's large magnetic moment, which is about three times that of the proton, and the availability of instrumentation capable of observing the relaxation of its spin soon after implantation, the muon spin relaxation technique is proving to be a powerful tool for studying the dynamics of magnetic ions. In a muon spin relaxation experiment, one can easily measure correlation times for random spin fluctuations in the range of 10^{-4} to 10^{-11} sec. This is true even if there is no applied magnetic field, something that is generally not true for other resonance techniques. Moreover, one can implant muons in any material of interest, including materials that cannot be studied by nmr. In all of the above studies, one can investigate the interaction between the positive muon and the host atoms free of probe–probe interactions, exploiting the fact the muons in the sample are always extremely dilute.

There are certainly also disadvantages to the technique. As a magnetic probe, the charge of the muon can perturb its environment significantly. (On the other hand, one can argue that this presents an interesting theoretical problem in simple metals, for example.) Also, despite the high sensitivity of the technique, the muon's short lifetime τ_μ of 2.2 microseconds and limits on experimental timing may yield linewidths inherently broader than those obtained in many magnetic resonance experiments. In addition, the muon may not live long enough to find its way to an equilibrium site in a solid, so identification of that site by infrared spectroscopy, for example, is not possible. The proton, with a lifetime of at least 10^{31} years, obviously does not have this problem. Similarly, the analysis of the products of chemical reactions, which can be important in establishing the pathways for those reac-

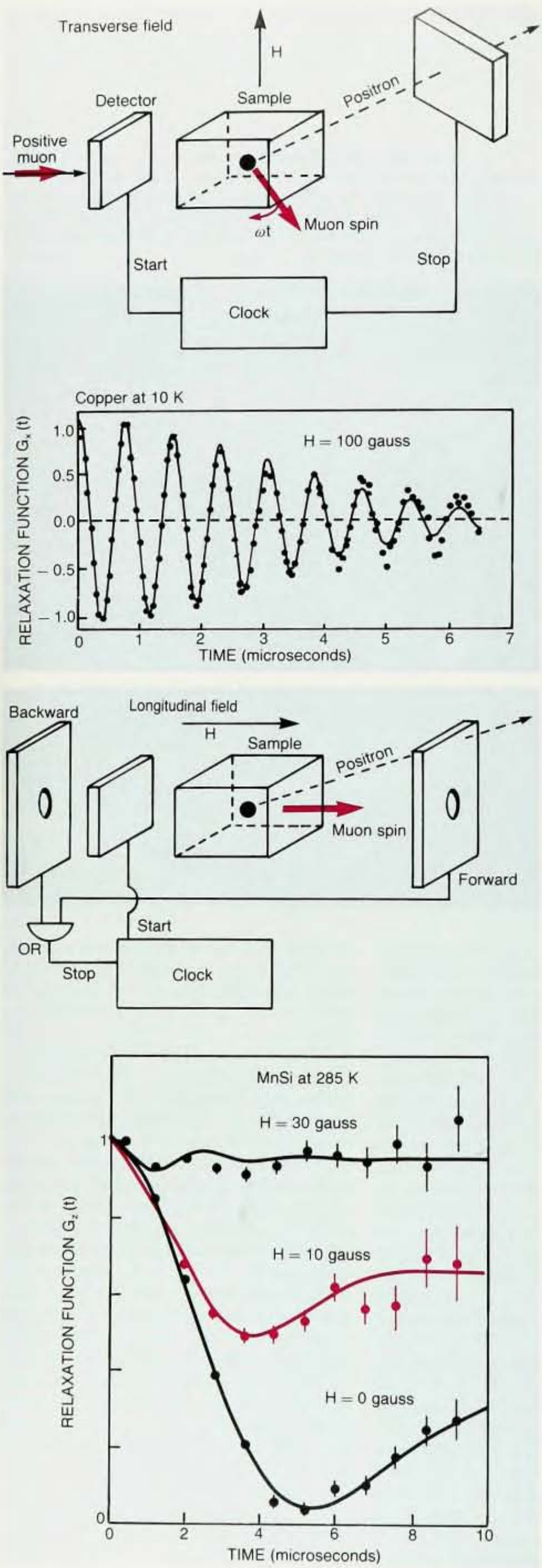

Spin detection schemes and corresponding results. In the setup illustrated at the left, the applied magnetic field is perpendicular to the spins (colored arrow) of the incident muons. In the configuration below, the two are parallel. In either case, the incident muon triggers a detector near the target sample and the decay positron triggers another counter, giving rise to time histograms such as those shown below the diagrams. (Copper data from TRIUMF; MnSi data from reference 7.) Figure 2

tions, is not feasible in muonium chemistry. Nevertheless, these points are often outweighed by the advantages inherent in this unusual probe.

The technique

Muons are created and destroyed in the weak-interaction sequence

$$\pi^+ \rightarrow \mu^+ \nu_\mu$$
$$\mu^+ \rightarrow e^+ \nu_e \bar{\nu}_\mu$$

The positive pion, which has a lifetime of 26 nsec, is initially produced by bombarding a suitably chosen target with high-energy protons. Because the pion has spin zero, conservation of angular momentum guarantees that the muon is produced 100% longitudinally polarized (left-handed) in the pion's rest frame. One can implant muon beams of high polarization and various energies in materials ranging in thickness from about 10 mg/cm^2 to 1 g/cm^2. The muon generally retains a significant degree of its polarization during the thermalization process.

After thermalization, one can monitor the loss of muon polarization because the positron is emitted preferentially along the muon's spin direction. Thus the positron counting rate N is represented by an equation of the form

$$dN(\theta,t) = 1/(4\pi\tau_\mu)\ e^{-t/\tau_\mu} \times [1+\Sigma A_\mu G_\mu(t) \cos\theta]\ d\Omega dt$$

The positron is emitted at an angle θ relative to the spin direction of the muon. The relaxation function $G_\mu(t)$ describes the loss of polarization in time. The summation indicates that, in general, the muon can experience more than one precession frequency, particularly in the case of the $\mu^+ - e^-$ interaction. The asymmetries A_μ are determined experimentally, and the sum

Relaxation of muon spins in copper as a function of time, with no applied magnetic field. The short-time Gaussian width σ_z remains roughly unchanged with temperature. The long-time damping, however, indicates more muon motion at high and low temperatures than at temperatures in between. The solid lines are chi-squared fits to the data. (From reference 13.) Figure 3

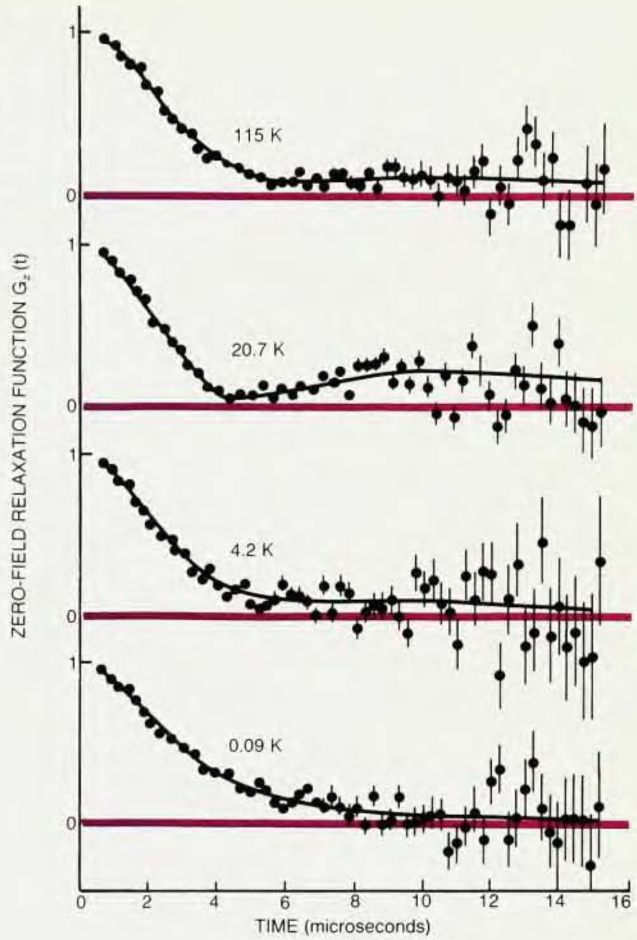

ΣA_μ is about 0.25.

In the "time differential" muon spin relaxation technique, an incident muon triggers a muon-counter telescope (a series of plastic scintillators), stops in the target and sometime later decays into a positron that triggers a similar counter array. Figure 2 illustrates the basic experimental arrangement. The incident muon starts a high-frequency "clock," which the positron stops. Typical systems record 10^6 to 10^7 events per hour. The detectable time interval between a start pulse and a stop pulse varies from a few nanoseconds to about 20 microseconds, the shortest time being dictated by the deadtime of the spectrometer and the longest by the lifetime of the muon. The basic rate limitation of the time-differential technique is that there can be no more than one muon at a time in the target, so as not to confuse events. One can overcome this limitation by measuring integrated responses to pulses of muons. An example of such an integral counting technique is the stroboscopic method developed at the Swiss Institute for Nuclear Research and used in conjunction with precise measurements of the local muon magnetic field or of the muon's magnetic moment.[2] In this method, one sets the muon's Larmor frequency equal to a multiple of the frequency at which muon pulses arrive from their cyclotron source. Then the spins of muons entering the target are synchronized with those already there, eliminating any confusion about the spin orientation of decaying muons.

By measuring the precessional frequency of the muons, one determines the time-averaged strength of the internal magnetic field at the sites where the muons come to rest. A site-to-site variation σ of static internal fields will cause a dephasing of the ensemble of muon spins and hence a loss of polarization, a phenomenon known as inhomogeneous broadening, or as a T_2 process in nmr. Likewise, time-varying transverse fields that fluctuate at the muon's local Larmor frequency will also bring about a loss of polarization by causing muons to undergo spin flips, a phenomenon known as spin–lattice relaxation, or as a T_1 process in nmr. Such dynamic fluctuations in the local field can be caused by the motion of muons or by the intrinsic time dependence of the local field itself. Random fluctuations are often described by a correlation time τ, which is the characteristic time for the field to change to a new value that shows no correlation with the original value. The relaxation function $G_\mu(t)$ is therefore dependent upon such parameters as the site-to-site variation σ in the magnetic field and the correlation time τ.

In a transverse applied magnetic field (usually defined as the x direction) the muon spin precesses in a plane perpendicular to the field with a certain Larmor frequency. In a 100-gauss field, for example, the precessional frequency is 1.355 MHz. As the muons precess, their decay asymmetry pattern sweeps past the counter telescope, giving rise to characteristic "wiggles" at the Larmor frequency ν. Such wiggles, which are described by the above equation with the angle θ given by $2\pi\nu t$, are shown in figure 2 for muons in copper at 10 K. Transverse-field studies cannot distinguish between the static and dynamic causes of relaxation discussed above.

In studies where the magnetic field is longitudinal or zero, the initial direction z of the muon's spin defines the nature of the muon spin relaxation time histogram. There are, in fact, two time distributions, each of the form of the above equation, with $\cos\theta = \pm 1$. Zero-field studies are particularly easy with muon spin relaxation techniques—compared to nmr, for example—because the muon spin is already polarized. In addition, relaxation with static and dynamic causes is often exhibited simultaneously. This is seen in the MnSi data in figure 2 and in the Cu data in figure 3; these data come from zero-field and longitudinal-field work[7] that was pioneered at the TRIUMF cyclotron. The short-time relaxation seen in $G_z(t)$ in figures 2 and 3 is due to

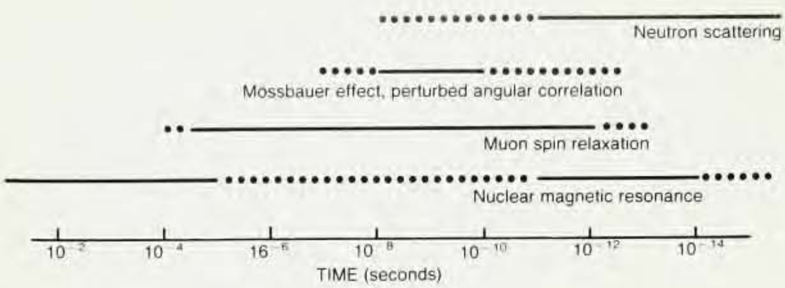

Ranges of electronic spin correlation times that one can obtain using various probes. The solid lines indicate correlation times τ that are usually measurable. The dotted lines indicate times measurable in favorable cases. Figure 4

transverse-field inhomogeneities. For the static zero-field case, the relaxation function $G_z(t)$ returns to $1/3$ at long times, because the z component of the local random field produces no relaxation. An applied longitudinal magnetic field can hold the muon polarization, as we see in the example of MnSi in a 30-gauss field. Slow fluctuations of the magnetic field, that is, fluctuations for which $\sigma\tau \gg 1$, cause the relaxation function to lose its $1/3$ component because the μ spins track the field. We see this in figure 3. For rapid fluctuations, for which $\sigma\tau \ll 1$, the form of the relaxation function $G_z(t)$ changes, losing its short-time decrease as the fluctuations average out the inhomogeneities in the field.

Muons in metals

Two themes underlie muon spin relaxation studies in metals: diffusion and magnetism. The muon's exceptionally small mass compared to that of the proton makes it a very sensitive probe of quantum tunneling, particularly at temperatures below 1 K, a regime that is not accessible to proton diffusion studies. In addition, one can monitor muons at infinite dilution, unlike hydrogen in most diffusion experiments. The use of muon spin relaxation to probe magnetic fields in solids can itself be divided into two broad categories: the use of transverse-field muon spin relaxation to study hyperfine fields and spin densities at interstitial sites, and the use of zero- and longitudinal-field muon spin relaxation to study field dynamics. Reference 8 is an excellent review of hyperfine-field studies, and reference 9 describes studies of interstitial spin densities. Here we concentrate on dynamical measurements.

Diffusion. The transverse-field relaxation rate for muons in copper is known[10,11] for temperatures ranging from a fraction of a degree above absolute zero to near 1000 K. In the temperature range between 10 K and 80 K, the measured relaxation function $G_x(t)$ is Gaussian, reflecting the nuclear dipole field distribution, and the relaxation rate is nearly constant, indicating that the muon is essentially immobile. We can determine the location of the muon because the distribution σ_x of local fields depends both on the muon site and on the strength and direction of the applied field relative to the crystal axes. The results[11] for copper at 80 K are consistent with an octahedral occupancy, assuming a small lattice dilation of about 5% due to the presence of the muon.

Above 80 K, the relaxation rate decreases monotonically until it reaches the lowest measurable value of about 0.01 per microsec at about 240 K. This decrease or line narrowing is due to muon motion, which has the effect of averaging out the dipole field variations to a greater and greater extent as the muon moves faster and faster.

The most interesting behavior is seen at low temperatures, where the line width again narrows. Recent zero-field studies at TRIUMF[12] and KEK[13] have shown that the static Gaussian field distribution σ_z remains constant below 5 K, but that the muon motion *increases* as the temperature *decreases*. Below about 0.7 K the hopping rate remains constant, but nonzero. This is illustrated in figure 3, where the damping of the long-time tail in the relaxation function $G_z(t)$ reflects muon motion both at low and high temperatures.[13] The curve at 20.7 K shows nearly static muons. The constant value of the distribution σ_z rules out drastic site changes at low temperatures such as would be seen in impurity trapping.

The mechanism for increased muon mobility at low temperatures is not yet understood, but tunneling is a likely process. Such quantum mechanical effects are limited by fluctuations in the site-to-site energy levels. These fluctuations are the result of lattice vibrations or crystal imperfections, which cause a distribution of interstitial energy levels. In the case of crystal imperfections, if the random shifts in energy levels are greater than the energy required for motion between sites, the muons become localized.[14] A possible explanation[12] of the strange temperature dependence of the muon's mobility is that muon motion is limited by thermal disorder above 5 K and by static distortions below about 0.5 K. Theories of coherent motion predict a very strong temperature dependence—as T^{-9}—in extreme contradiction to the data, which show a $T^{-0.7}$ dependence.[10] A recent suggestion[15] is that scattering of conduction electrons by muons at low temperatures can cause a minimum in the rate at which muons hop.

Magnetic ions in metals. Dilute magnetic systems formed by dissolving magnetic ions such as manganese or iron in copper, silver or gold illustrate the power of the muon spin resonance technique for studying spin dynamics. These materials have been given the name "spin-glasses," because at low temperatures the magnetic ions are nearly frozen in apparent random orientations, in contrast to ferromagnets or antiferromagnets, which have long-range spatial order.[16] This freezing behavior is reflected by a cusp in the ac susceptibility at the glass transition temperature T_g. This susceptibility is a measure of the tendency of the spin system to follow changes in a small applied magnetic field. At the same time, with no applied field there is no macroscopic magnetization. A question of considerable interest today in the study of spin glasses involves the nature of the freezing transition; interest is heightened by the belief that spin glasses are exemplary systems in which to study the characteristics of phase transitions in disordered materials.

The current interest in using muon spin relaxation as a technique to study spin glasses is predicated on two important points. First, as figure 4 illus-

Temperature dependence of the magnetic ion correlation time (right-hand data and scale) and the static-field distribution parameter (left-hand data and scale) for several representative metallic spin glasses. The data are from LAMPF[18] and TRIUMF[17] and are scaled by the glass transition temperatures for each material. The lines are to guide the eye. Figure 5

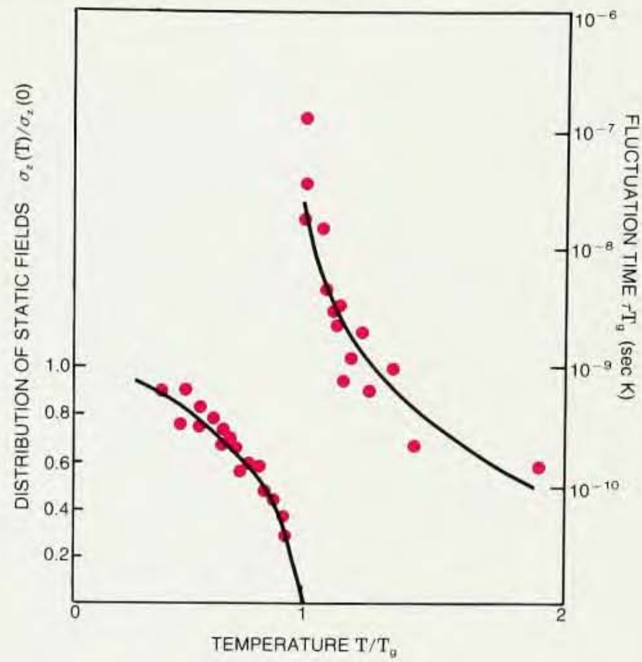

trates, the technique provides information about spin fluctuations in a time domain often inaccessible to older techniques such as neutron scattering, Mössbauer effect measurements and nuclear magnetic resonance. Second, the fact that one can carry out muon spin relaxation measurements with virtually no applied field is an important advantage, because even fields of a few hundred gauss have been shown to perturb the transition to a spin glass. Other magnetic resonance techniques often require an applied field.

The right-hand curve in figure 5 shows zero-field dynamical measurements made at TRIUMF[17] and LAMPF[18] in several common spin-glass materials. One sees that the data scale reasonably well by the glass transition temperature, and that there is a very rapid lengthening of the spin fluctuation time as one approaches the glass transition temperature from above, indicating the onset of freezing. The temperature dependence of the correlation time τ is well described[17,18] by the relation $\tau \propto (T/T_g - 1)^{-2}$. Some early models[16] of spin-glass dynamics, based on noninteracting clusters of spins, predicted a correlation time τ proportional to $\exp(E/T)$, where E is an energy barrier for cluster rotation. Because the measured correlation time changes so rapidly, these early models would yield an energy barrier E twenty times the glass temperature T_g, an unphysically large value. Different models,[16] in which evanescent clusters interact and grow in size as the temperature is lowered, or in which each individual spin tends to align itself along a local direction of minimum energy, are more consistent with the data.

Just below the glass transition temperature, the distribution σ_z of static fields becomes nonzero, and for much lower temperatures increases to a value near the frozen-spin value (figure 5). Because the macroscopic magnetization remains at zero for temperatures below that of the glass transition, the spins must be freezing in random orientations as the temperature is lowered. The monotonic increase of the distribution σ_z of static fields occurs because the amplitudes of the spin fluctuations decrease as the material is cooled.

One way to characterize the dynamical behavior of a many-body system is with the energy distribution of fluctuations as a function of frequency ω. We denote this power density as $J(\omega)$. In simple theoretical models for nonrandom spin systems, such as ordinary ferromagnets, the power density is Lorentzian, that is, $J(\omega)$ has the form $1/(\omega^2 + \Gamma^2)$, where Γ is a constant. Taking the Fourier transform of the power density $J(\omega)$ shows that this corresponds to an exponential correlation function in time. In disordered systems, however, one expects[19] the density of modes to show a power-law behavior. It is thus of great interest to look for this distinction experimentally.

When a muon is in a longitudinal applied field, internal transverse fields fluctuating at the muon's Larmor frequency ω_μ can cause its spin to flip between Zeeman levels. The degree of muon spin relaxation then depends upon the power density $J(\omega_\mu)$. Thus one can use the longitudinal-field dependence of the muon spin relaxation rate to map the power density $J(\omega)$, provided that the applied field does not itself perturb the spin dynamics. For modest fields, this assumption is a good one at temperatures well below that of the glass transition.

Recent data taken at LAMPF for spin glasses of manganese ions in silver show[18] for the first time that the density of modes $J(\omega)$ is indeed given by a power law, reflecting the fundamental effects of disorder on the dynamics. One finds $J(\omega)$ proportional to $\omega^{\gamma-1}$, where γ is approximately $\frac{1}{2}$, in the frequency range of about 1 to 100 MHz. This behavior of the density of modes is in agreement with that predicted[16,19] by idealized models of simple spin glasses, and is consistent with neutron scattering data[18] that reflect spin-glass dynamics in the frequency range 10^3 to 10^6 MHz.

Muonium

When a positive muon thermalizes in matter, it is frequently through formation of a muonium atom. In gases, we can understand this mechanism qualitatively in terms of charge exchange, in which the muon acts like a proton and picks up an electron from a gas molecule.[3] In condensed phases, however, the mechanism for this process is still under active investigation,[4] because muonium seems to form readily in some materials but not at all in others. However muonium is formed, there are currently many investigations of its interactions in matter. In the general area of physical chemistry, for example, the light mass of the muonium atom allows the study of isotope effects at the most sensitive end of the atomic mass scale.[3,4,6] Like the hydrogen atom, muonium forms the most elementary type of defect in solids. The study of muonium in semiconductors such as silicon and germanium is particularly rewarding because no direct hydrogen electron paramagnetic resonance signals have ever been seen in these most industrially important semiconductors.

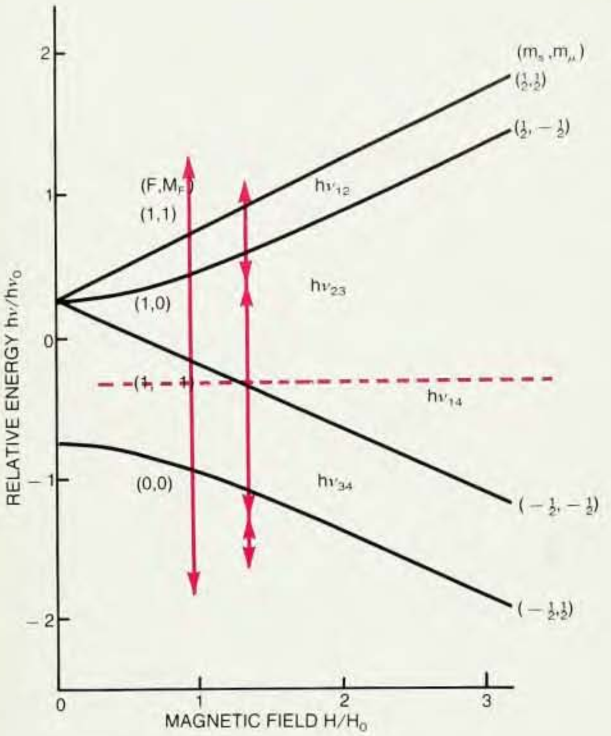

Breit–Rabi diagram for the eigenenergies of muonium in an applied field in a vacuum. At low fields, total-angular-momentum quantum numbers F and M_F describe the system. At high fields, the muon and electron spins are decoupled and the individual quantum numbers m_s and m_μ describe the system. The applied field is given in units of H_0, which is 1585 gauss. The frequency ν_0 is 4463 MHz. Figure 6

The interaction between the magnetic moment of the muon and the magnetic moment of the electron is known as a hyperfine interaction. This interaction is described by the Breit–Rabi Hamiltonian, which has hyperfine terms due to the coupling between the particles' spin, as well as terms due to the interaction of the spins and an external magnetic field. Figure 6 is the familiar energy-level diagram corresponding to the characteristic energies of this operator for an isotropic interaction of the muon and electron magnetic moments. The states of the polarization of the muon in muonium give rise to four allowed transitions, which are analogous to the allowed magnetic dipole transitions of the muon spin. At low magnetic fields, the transitions ν_{12} and ν_{23} appear clearly in the Fourier transform power spectrum, as figure 7a shows for muons in fused quartz in a 100-gauss applied field.[20] With high-time-resolution spectroscopy, it is also possible to observe[21] the high-frequency transitions ν_{14} and ν_{34}, which are both approximately the same as the 4463 MHz transition ν_0 of vacuum muonium in zero field.

Generally, hydrogen in noncubic insulators exhibits a weakly anisotropic hyperfine interaction of energy $h\nu_0$, where the frequency ν_0 is close to the free hydrogen value of 1420 MHz. Muonium shows[22] this kind of interaction in α-quartz, single-crystal ice, and a variety of other insulators. The situation is different in semiconductors, however, as one can easily see in the Fourier transforms shown in figure 7, which compare p-type silicon with fused quartz.[20] In quartz, as well as in silicon, the muonium frequencies ν_{12} and ν_{23} are clearly visible, centered at 140 MHz. In quartz, these frequencies yield a hyperfine interaction strength quite close to the vacuum value ν_0. In silicon, however, the larger splitting near 140 MHz corresponds to 0.45 ν_0. Similar large splittings seen in germanium, and more recently in diamond, have stimulated much theoretical effort. These splittings indicate a marked reduction in the electron spin density around the muon. The two predominant peaks near 45 MHz in silicon correspond to what has been called "anomalous" muonium. These data, which were taken at the Berkeley cyclotron more than a decade ago, represent some of the earliest muon spin relaxation measurements. Modern-day spectra show an improved signal-to-noise ratio of about 100.

One way to measure the asymmetry of the electron distribution around a muon in a solid is to consider the strengths of the muon–electron hyperfine interaction perpendicular to and parallel to a symmetry axis. Experiments conducted primarily at SIN show[23] that the anomalous muonium state is described with high precision by the axially symmetric Breit–Rabi Hamiltonian, with the axis of symmetry along any of the four $\langle 111 \rangle$ axes of the crystal. The ratio of the energies associated with the parallel and perpendicular components of the interaction varies from about 2.3 in diamond to about 5.5 in silicon. Also, the magnitude of the interaction is reduced by a factor of 10 to 30 compared to the vacuum value, suggesting an extended defect state in which the muonium electron extends over many lattice sites.

These data raise a number of interesting questions about the electronic structure of simple defect states in elementary semiconductors. Yet to be explained are the small but highly anisotropic hyperfine interactions of anomalous muonium and the abundance of muonium and anomalous muonium, despite the lack of analogous electron paramagnetic resonance signals for hydrogen in these materials. Experiments to date, including the channeling[24] of positrons and muons along crystal axes in semiconductors, indicate that muonium occupies a tetrahedral site at low temperatures but becomes mobile, possibly even changing into anomalous muonium, at high temperatures. One likely site for anomalous muonium is a host atom vacancy, but despite considerable theoretical effort, the site remains uncertain. Finally, it may be that anomalous muonium is a thermodynamically metastable state; this could explain the absence of hydrogen electron paramagnetic resonance signals in these materials.

Prospects

The utilization of parity-violating muon decay for the study of condensed-

Power spectra. The spectrum for muons in quartz was taken at room temperature in a 100 gauss magnetic field. It shows the two triplet-spin muonium transitions ν_{12} and ν_{23}. The peak at very low frequency is due to the precession of free muons in the applied field. The spectrum for muons in silicon was taken at 77 K in a 100 gauss field. The two lines near 140 MHz are the isotropic muonium state, analogous to muonium in quartz. The lines near 45 MHz are from the anisotropic anomalous muonium state. The small peak at 19 MHz is an artifact due to rf structure in the cyclotron beam. (From ref. 20.) Figure 7

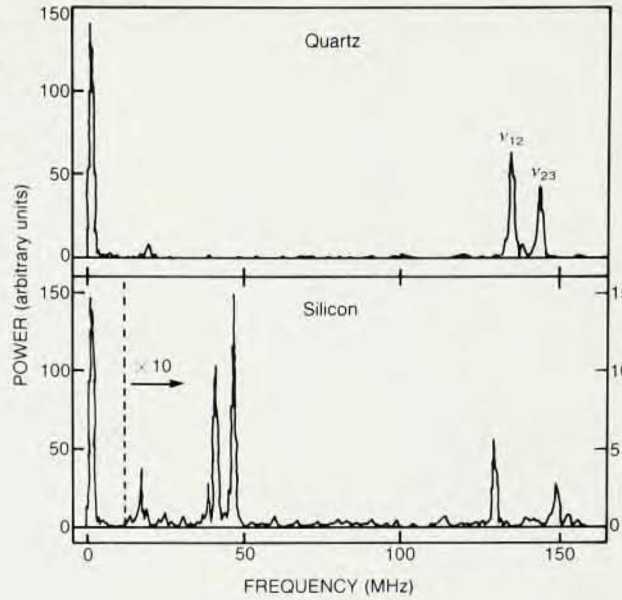

matter physics is a beautiful example of the interplay between esoteric scientific pursuits in one field and their ensuing applications in other fields. Today the muon spin-relaxation technique is attracting more and more attention from both solid-state physicists and physical chemists, and this trend shows no sign of abating. Where does the field go from here? There is no question that the muon is, in many ways, a unique probe of matter, but a technique's uniqueness is not sufficient to guarantee its longevity. Its continued use in exploration at the frontiers of science is essential. There are many examples of this use of muon spin relaxation, some of which we have discussed in this article—quantum diffusion and localization, magnetic ion dynamics, and defect studies in semiconductors. Many other examples come to mind, such as determination of the role of tunneling in chemical reaction dynamics; analysis of the initial stages of radiolysis, processes in which charged particles slow down by creating ionization; and zero-field studies of phase transitions, where nuclear magnetic resonance may not be feasible. Preliminary studies of muonium in quartz powders indicate[6] that muonium may diffuse to the surface and thereby become an unusual probe of surface physics phenomena.

New experimental methods are also essential for the continued success of any technique. One example of a new method in muon spin relaxation is the use of sharply pulsed muon beams. This can have two important effects. First, the rate limitations inherent in the usual time-differential technique disappear because all of the muons in a given pulse arrive together, within the beam pulse width, producing a single timing signal. Second, experiments on pulsed systems become possible by synchronizing the pulses of the muon beam and those of the system under study; experiments on the resonant flipping of muon spins and on systems involving pulsed lasers are two examples. Lasers could be used to study reactions involving excited states or optical transitions of muonium in solids. The first investigations of the resonant flipping of muon spins using a pulsed beam are now complete, having been undertaken[6] at KEK, in Japan. More applications are sure to follow as the knowledge of the technique becomes more widespread.

* * *

We would like to acknowledge the contributions of the muon spin relaxation community at large, and particularly Tom Estle for his input to the section on muonium. Donald Fleming would like to express his appreciation to the John Simon Guggenheim Foundation for its support of a sabbatical year at the Max Planck Institut Für Strömungsforschung, Göttingen, West Germany.

References

1. J. H. Brewer, K. M. Crowe in *Muon Physics*, Vol. III, V. Hughes, C. S. Wu, eds., Academic, New York (1975); J. H. Brewer, K. M. Crowe, Ann. Rev. Nucl. Sci. **28**, 239 (1978); National Research Council, *Muon Sources for Solid-State Reseach*, National Academy, Washington, D.C. (1984).
2. A. Schenck in *Nuclear and Particle Physics at Intermediate Energies*, J. B. Warren, ed., Plenum, New York (1976), p. 159; E. Klempt, R. Schulze, H. Wolf, M. Camani, F. N. Gygax, W. Rüegg, A. Schenck, H. Schilling, Phys. Rev. D **25**, 652 (1982).
3. D. G. Fleming, R. J. Mikula, D. M. Garner, Phys. Rev. A **26**, 2527 (1982); D. G. Fleming, Proc. XII ICPEAC, North Holland, Amsterdam (1981), p. 297.
4. P. W. Percival, Radiochimica Acta **26**, 1 (1979); D. C. Walker, *Muon and Muonium Chemistry*, Cambridge U.P. (1983).
5. A. Seeger in *Hydrogen in Metals*, G. Alefeld, J. Völkl, eds., Springer-Verlag Berlin (1978), p. 349.
6. For general information consult proceedings of the three topical muon spin relaxation conferences: Hyperfine Interactions **6** (1979); Hyperfine Interactions **8** (1981); Hyperfine Interactions **17–19** (1984).
7. R. S. Hayano, Y. J. Uemura, J. Imazato, N. Nishida, T. Yamazaki, R. Kubo, Phys. Rev. B **20**, 850 (1979).
8. A. B. Denison, H. Graf, W. Kündig, P. F. Meier, Helvetica Physica Acta **52**, 460 (1979); S. Estreicher, P. F. Meier, Phys. Rev. B **25**, 297 (1982).
9. A. Schenck, Helvetica Physica Acta **54**, 471 (1981); W. Studer, F. N. Gygax, A. Hintermann, W. Rüegg, A. Schenck, A. J. Van Der Wal, Hyperfine Interactions **17–19**, 299 (1984).
10. K. W. Kehr, D. Richter, J.-M. Welter, O. Hartmann, E. Karlsson, L. O. Norlin, T. O. Niinikowski, A. Yaouanc, Phys. Rev. B **26**, 567 (1982); J.-M. Welter, D. Richter, R. Hempelmann, O. Hartmann, E. Karlsson, L. O. Norlin, T. O. Niini-

kowski, D. Lenz, Z. Phys. B **52**, 303 (1983).

11. M. Camani, F. N. Gygax, W. Rüegg, A. Schenck, H. Schilling, Phys. Rev. Lett. **39**, 836 (1977); O. Hartmann, Phys. Rev. Lett. **39**, 832 (1977).
12. C. W. Clawson, K. M. Crowe, S. S. Rosenblum, S. E. Kohn, C. Y. Huang, J. L. Smith, J. H. Brewer, Phys. Rev. Lett. **51**, 114 (1983).
13. R. Kadono, J. Imazato, K. Nishiyama, K. Nagamine, T. Yamazaki, D. Richter, J. M. Welter, Yamada Conf. Muon Spin Rotation, Hyperfine Interactions **17–19**, 109 (1984).
14. P. W. Anderson, Phys. Rev. **109**, 1492 (1958).
15. J. Kondo, Proceedings of the 17th Conference on Low Temperature Physics, Karlsruhe, Germany, August 1984.
16. For a recent review of spin-glass theories see K. H. Fischer, Phys. Status Solidi B **116**, 357 (1983). For general reviews of spin-glass experiments, see J. A. Mydosh in *Disordered Systems and Localization*, J. Ehlers, ed., Springer-Verlag, Berlin (1981), p. 87.
17. Y. J. Uemura, T. Yamazaki, R. S. Hayano, R. Nakai, C. Y. Huang, Phys. Rev. Let. **45**, 583 (1980); Y. J. Uemura, T. Yamazaki, J. Magn. Magn. Mat. **31–34**, 1359 (1983); Y. J. Uemura, T. Yamazaki, D. R. Harshman, M. Senba, J. H. Brewer, E. Ansaldo, R. Keitel, Hyperfine Interactions **17–19**, 453 (1984); Y. J. Uemura, Hyperfine Interactions **17–19**, 447 (1984).
18. R. H. Heffner, M. Leon, M. E. Schillaci, D. E. MacLaughlin, S. A. Dodds, J. Appl. Phys. **53**, 2174 (1982); D. E. MacLaughlin, L. C. Gupta, D. W. Cooke, R. H. Heffner, M. Leon, M. E. Schillaci, Phys. Rev. Lett. **51**, 927 (1983); R. H. Heffner, D. E. MacLaughlin, Phys. Rev. B **29**, 6048 (1984).
19. H. Sompolinsky, A. Zippelius, Phys. Rev. Lett. **47**, 359 (1981), Phys. Rev. B **25**, 6860 (1982); J. Phys. C**40**, L1059 (1982).
20. J. H. Brewer, K. M. Crowe, F. N. Gygax, R. F. Johnson, B. D. Patterson, D. G. Fleming, A. Schenck, Phys. Rev. Lett. **31**, 143 (1973).
21. E. Holzschuh, W. Kündig, B. D. Patterson, Helv. Phys. Acta **54**, 552 (1982).
22. J. H. Brewer, D. G. Fleming, D. P. Spencer in *Nuclear and Electrical Resonance Spectroscopies Applied to Materials Science*, E. N. Kaufmann, G. K. Shenoy, eds. Elsevier North Holland, New York (1981), p. 487; P. W. Percival, J. C. Brodovitch, K. E. Newman, D. P. Spencer, Chem. Phys. Lett. **93**, 366 (1982); D. P. Spencer, D. G. Fleming, J. H. Brewer, Hyperfine Interactions **17–19**, 567 (1984).
23. B. D. Patterson, Hyperfine Interactions **17–19**, 517 (1984); E. Holzschuh, W. Kündig, P. F. Meier, B. D. Patterson, J. P. F. Sellschop, M. C. Stemmet, H. Appel, Phys. Rev. A **25**, 1272 (1982); E. Holzschuh, H. Graf, E. Recknagel, S. Weidinger, Th. Wickert, P. F. Meier, Phys. Rev. B **20**, 4391 (1979).
24. B. D. Patterson, A. Bosshard, U. Straumann, P. Truöl, A. Wüest, Th. Wichert, Phys. Rev. Lett. **52**, 938 (1984); K. Maier, Hyperfine Interactions **17–19**, 3 (1984). □